ELSEVIER

Journal of Alloys and Compounds 451 (2008) 128–131

Journal of ALLOYS AND COMPOUNDS

www.elsevier.com/locate/jallcom

Red-luminescence analysis of Pr^{3+} doped fluoride crystals

S. Khiari [a], M. Velazquez [a], R. Moncorgé [a], J.L. Doualan [a], P. Camy [a], A. Ferrier [a,*], M. Diaf [b]

[a] *Centre Interdisciplinaire de Recherche Ions et Lasers, UMR 6637 CNRS-CEA-ENSICAEN, 6 Boulevard Maréchal Juin, 14050 Caen, France*

[b] *Département de Physique, Université Badji Mokhtar, BP 12, 23000 Annaba, Algeria*

Available online 21 April 2007

Abstract

We report here on the absorption and fluorescence properties of the Pr^{3+} doped crystals $LiYF_4$, BaY_2F_8, KY_3F_{10}, KYF_4 and CaF_2 emphasizing on their characteristics in the visible domain for blue-diode pumped laser operation around 605 nm.

Keywords: Optical materials; Luminescence; Praseodymium; Fluoride; Laser

1. Introduction

Pr^{3+} doped fluoride and oxide crystals and glasses are being studied since a long time [1] for their UV emissions for scintillator and broad band laser applications, their visible ones for multicolor lasers in high definition TV and medical applications, and their near-infrared one for fiber optics communications. However, except for some (Yb^{3+}, Pr^{3+}) doped systems in which excitation was achieved with the aid of commercially available and compact near-infrared laser diodes, most of the singly doped systems have worked under non-optimized and/or bulky excitation pump sources such as flash-lamps or argon-ion lasers. This situation may rapidly change, however, due to the recent appearance and the future improvement of diode lasers operating around 440 nm, thus which can be used to directly pump the $^3P_{0,1,2}$ emitting levels of the Pr^{3+} ions, and the recently proved laser operation of a Pr:$LiYF_4$ single crystal and a Pr:ZBLAN glass fiber by using such a diode laser with only a few mW pump power [2,3]. This opens the way to various types of laser systems working CW as well as in the picosecond regime at specific laser wavelengths for various applications. This is the reason why we recently revisited some of the Pr^{3+} doped fluoride materials which were considered in the past but for which some crucial spectroscopic parameters (Judd–Ofelt parameters, radiative lifetimes and branching ratios, absorption and emission cross-sections) were missing in the literature, and why we investigated some new ones.

2. Absorption spectra and Judd–Ofelt analysis

Six crystals have been grown and studied: 0.26%Pr:$LiYF_4$, 0.1%Pr:BaY_2F_8, 0.35%Pr:KY_3F_{10}, 0.5%Pr:KYF_4 and 2.8%Pr:CaF_2. Their room temperature absorption spectra were recorded within the three following spectral ranges: (i) from 420 to 500 nm, in the region of the $^3H_4 \rightarrow {}^3P_0$ (around 480 nm), $^3H_4 \rightarrow {}^3P_1$, $^1I_6$ (around 470 nm) and $^3H_4 \rightarrow {}^3P_2$ (around 445 nm) absorption transitions; (ii) from 550 to 640 nm, in the region of the $^3H_4 \rightarrow {}^1D_2$ transition; and (iii) from 1200 to 2500 nm, in the region of the $^3H_4 \rightarrow {}^3F_3$, $^3F_4$ (around 1500 nm), $^3H_4 \rightarrow {}^3F_2$ (around 2000 nm) and $^3H_4 \rightarrow {}^3H_6$ (around 2250 nm). All these spectra have been analysed by using the Judd–Ofelt (JO) method and the matrix elements given in Ref. [4]. We did not use any modified procedure as was suggested in the past [5,6]. The fit to the data was indeed found quite acceptable just by omitting the data for the $^3H_4 \rightarrow {}^3P_2$ transition and by treating together the data for the $^3H_4 \rightarrow {}^3P_1$ and $^1I_6$ transitions, on one hand, and the data for the $^3H_4 \rightarrow {}^3F_3$ and $^3F_4$ transitions, on the other hand. The resulting JO parameters are reported in Table 1. The table also contains the derived intrinsic radiative lifetime τ_{int} for the $^3P_0$ emitting level and the branching ratio for the $^3P_0 \rightarrow {}^3H_6$ emission transition around 605 nm for the various systems. The optical density spectra corresponding to the $^3H_4 \rightarrow {}^3P_2$ transition around 445 nm are reported in Figs. 1–4 and the absorp-

* Corresponding author.
E-mail address: alban.ferrier@ensicaen.fr (A. Ferrier).

0925-8388/$ – see front matter © 2007 Elsevier B.V. All rights reserved.
doi:10.1016/j.jallcom.2007.04.233

Table 1
$^3H_4 \rightarrow {}^3P_2$ absorption cross-section around 445 nm, JO parameters, branching ratio, fluorescence/effective and radiative lifetimes, and emission cross-section around 607 nm for the $^3P_0 \rightarrow {}^3H_6$ transition for the various Pr doped materials

Studied crystals	$^3H_4 \rightarrow {}^3P_2$ max absorption cross-section and wavelength	Judd–Ofelt parameters (Ω_2, Ω_4, Ω_6) (10^{-20} cm^2)	$^3P_0 \rightarrow {}^3H_6$ red emission branching ratio	$^3P_0$ fluorescence/effective/intrinsic radiative lifetimes, $\tau_f/\tau_{eff}/\tau_{int}$ (μs)	$^3P_0 \rightarrow {}^3H_6$ max emission cross-section and wavelength
$LiYF_4$: 0.26%Pr	8×10^{-20} cm^2, 443.4 nm (E//c)	3.45, 3.94, 6.13	0.15	50/53/37	2.8×10^{-19} cm^2, 604.2 nm (E//c)
BaY_2F_8: 0.1%Pr	3.7×10^{-20} cm^2, 444.5 nm (E//b)	0.18, 4.45, 3.31	0.10	50/77/49	1.25×10^{-19} cm^2, 607 nm (E//b)
KY_3F_{10}: 0.4%Pr	7.4×10^{-20} cm^2, 446 nm	1.43, 8.73, 16.63	0.22	34/30/24	1.9×10^{-19} cm^2, 610.1 nm
CaF_2: 2.8%Pr	0.7×10^{-20} cm^2, 443 nm	1.15, 3.60, 10	0.28	45/56/45	2.3×10^{-20} cm^2, 608 nm
KYF_4: 0.5%Pr	1.8×10^{-20} cm^2, 441.8 nm	3.92, 1.78, 7.94	0.24	60/72/54	9×10^{-20} cm^2, 605.3 nm

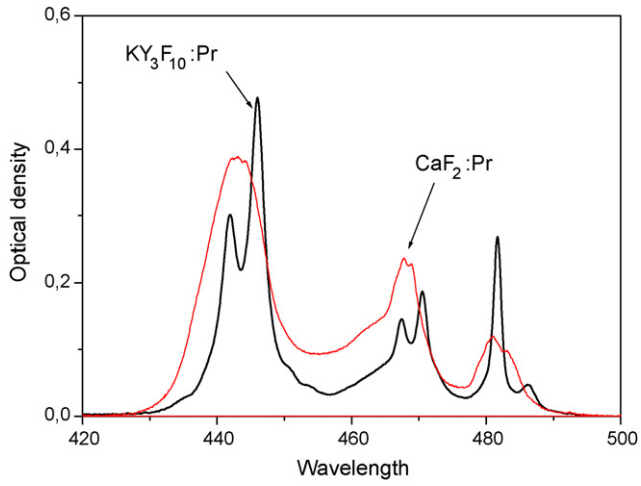

Fig. 1. Room temperature absorption spectra of Pr:KY_3F_{10} (thickness 2.38 mm) and Pr:CaF_2 (thickness 1.9 mm) around 445 nm.

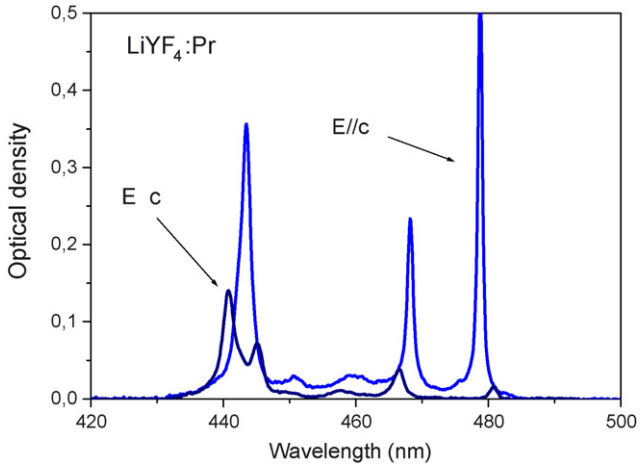

Fig. 2. Room temperature polarized absorption spectra of Pr:$LiYF_4$ (thickness 2.72 mm) around 445 nm.

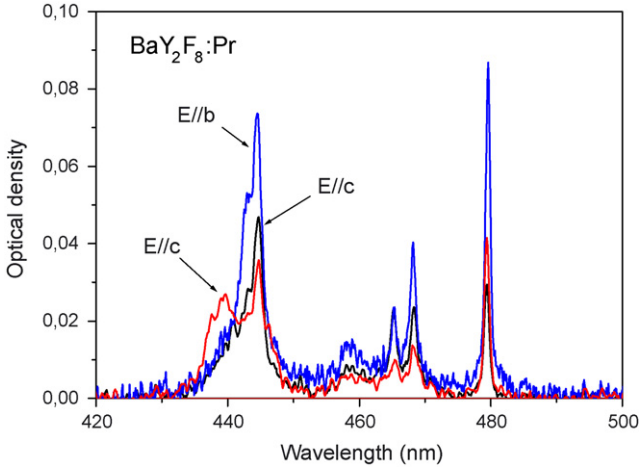

Fig. 3. Room temperature polarized absorption spectra of Pr:BaY_2F_8 (thickness 3.4 mm) around 445 nm.

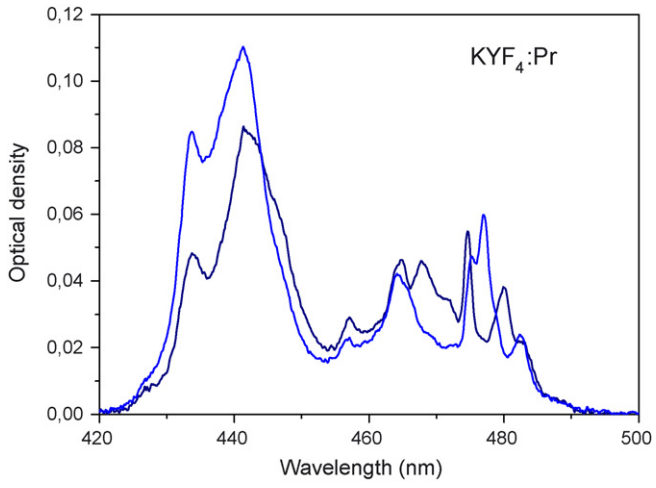

Fig. 4. Room temperature polarized absorption spectra of Pr:KYF_4 (thickness 2.74 mm) around 445 nm.

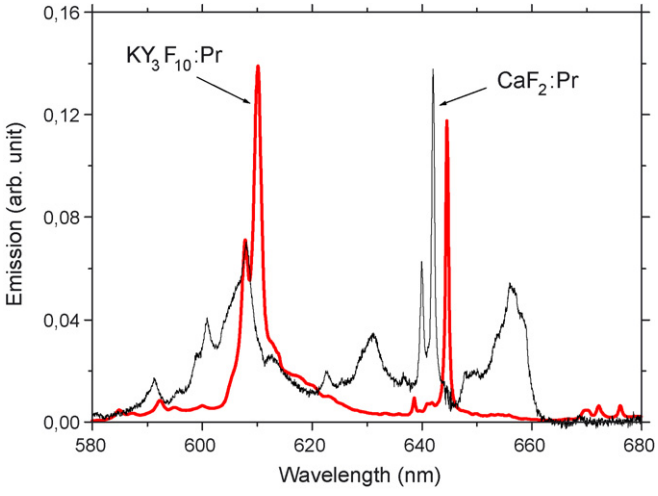

Fig. 5. Room temperature emission spectra of Pr:KY_3F_{10} and Pr:CaF_2 around 610 nm.

tion cross-sections at the wavelengths of the absorption peaks in Table 1.

3. Emission spectra and fluorescence decays

The emission spectra have been registered between 580 and 680 nm and reported in Figs. 5–8. These spectra are associated with emission transitions from the thermalized $^3P_1$, $^1I_6$ and $^3P_0$ levels to the $^3H_6$ and $^3F_2$ levels, around 605 and 640 nm, respectively. Due to the overlap of these transitions, their calibration in unit of emission cross-section is not easy. This has been done, however, for the emission peak around 605 nm, by approximating the usual Fuchtbauer–Ladenburg formula, as follows:

$$\sigma^{\mathrm{p}}_{I\to J}(\lambda) = \frac{3\lambda^5 A_{IJ}}{8\pi c n_p^2} \frac{I^p_{\mathrm{em}}(\lambda)}{\sum_p \int \lambda I^p_{\mathrm{em}}(\lambda)\,\mathrm{d}\lambda} \approx \frac{3\lambda^2 \beta_p \beta_{IJ}}{4\pi^2 n_p^2 \tau_{\mathrm{eff}} \Delta\upsilon} \qquad (1)$$

where $\beta_p \approx I^p_{\mathrm{em}}(\lambda)/\sum_p I^p_{\mathrm{em}}(\lambda)$ stands for the intensity ratio for a certain polarization p at the wavelength λ, β_{IJ} for the branching ratio for the considered inter-multiplet transition and τ_{eff} for the

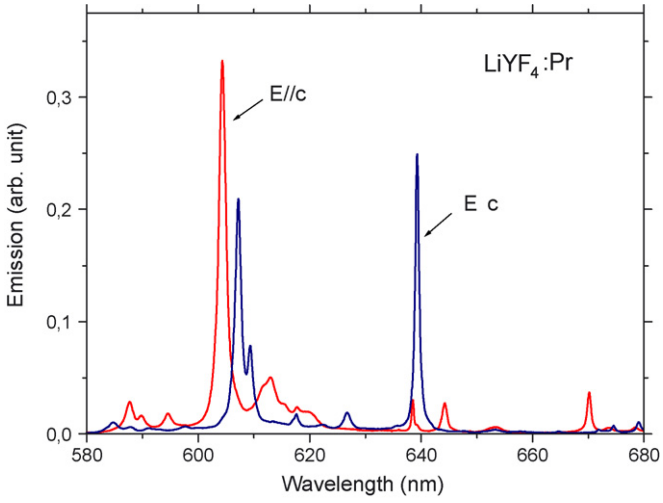

Fig. 6. Room temperature polarized emission spectra of Pr:$LiYF_4$ around 610 nm.

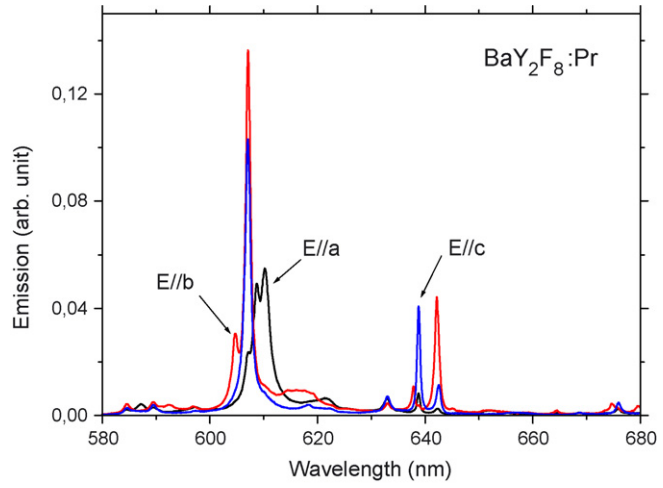

Fig. 7. Room temperature polarized emission spectra of Pr:BaY_2F_8 around 610 nm.

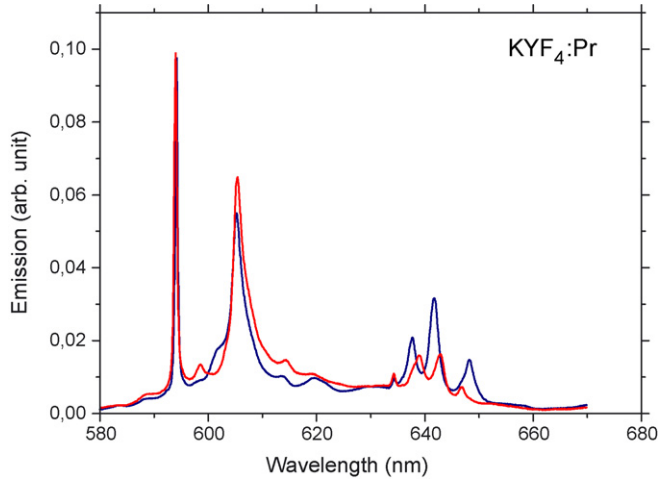

Fig. 8. Room temperature polarized emission spectra of Pr:KYF_4 and around 610 nm.

effective emission lifetime accounting for the thermalization of the $^3P_1$, $^1I_6$ and $^3P_0$ levels and which is given by the expression:

$$\tau_{\text{eff}} = \frac{g_{^3P_0} + (g_{^3P_1} + g_{^1I_6})\exp(-\Delta E/kT)}{g_{^3P_0}\sum_{J'} A_{^3P_0 \to J'} + \left(g_{^3P_1}\sum_{J'} A_{^3P_1 \to J'} + g_{^1I_6}\sum_{J'} A_{^1I_6 \to J'}\right)\exp(-\Delta E/kT)} \quad (2)$$

where the g's are the degeneracies of the levels and the A's the inter-multiplet transition probabilities derived from the JO analysis.

The τ_{eff} values, the measured fluorescence lifetimes τ_f as well as the resulting emission cross-sections at the wavelengths of the emission peaks are reported in Table 1. It is worth noting that the room temperature effective lifetimes τ_{eff} are always found larger than the intrinsic radiative lifetimes τ_{int} of the only $^3P_0$ level. This is expected from expression (2) which indicates that τ_{eff} is an increasing function of temperature. Moreover, most of the values for the fluorescence lifetimes τ_f measured at room temperature are found between the τ_{eff} and τ_{int} theoretical ones; this is in favour of our JO analysis.

4. Conclusion

The present study indicates that for laser operation around 605 nm under blue-diode laser pumping around 445 nm, the most suitable materials, in terms of laser threshold and laser efficiency, should be, by decreasing order: $LiYF_4$, KY_3F_{10}, BaY_2F_8, KYF_4 and CaF_2. Nevertheless, the systems KY_3F_{10} and KYF_4, because of their broad and reasonably strong emission transitions, might be very interesting for tunable and/or picosecond laser operation.

Acknowledgments

Thanks are expressed to AUF (Association Universitaire de la Francophonie) for allowing one of us (SK) from the University of Annaba (Algeria) to work in our CIRIL laboratory.

References

[1] R. Moncorgé, L.D. Merkle, B. Zandi, MRS Bull. (1999) 21–26, and references therein.
[2] A. Richter, E. Heumann, E. Osiac, G. Huber, W. Seelert, A. Diening, Opt. Lett. 29 (22) (2004) 2638–2640.
[3] A. Richter, E. Osiac, H. Scheife, E. Heumann, G. Huber, W. Seelert, A. Diening, Conference on Lasers and Electro-Optics (CLEO) 2005, paper CMAA4.
[4] M.J. Weber, J. Chem. Phys. 48 (10) (1968) 4774–4780.
[5] E. Dunina, A.A. Kaminski, A.A. Kornienko, K. Kurbanov, K.K. Pukhov, Sov. Phys. Solid State 32 (1990) 920.
[6] R.S. Quimby, W.J. Minicalco, J. Appl. Phys. 75 (1994) 613.